Fused heterocyclic compounds bearing bridgehead nitrogen as potent HIV-1 NNRTIs. Part 1: Design, synthesis and biological evaluation of novel 5,7-disubstituted pyrazolo[1,5-a]pyrim...

ARTICLE *in* BIOORGANIC & MEDICINAL CHEMISTRY · APRIL 2014

Impact Factor: 2.79 · DOI: 10.1016/j.bmc.2014.02.029

Accepted Manuscript

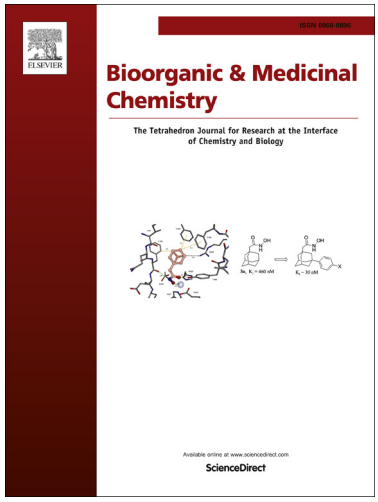

Fused heterocyclic compounds bearing bridgehead nitrogen as potent HIV-1 NNRTIs. Part 1: Design, synthesis and biological evaluation of novel 5,7-disubstituted pyrazolo[1,5-*a*]pyrimidine derivatives

Ye Tian, Deping Du, Diwakar Rai, Liu Wang, Huiqing Liu, Peng Zhan, Erik De Clercq, Christophe Pannecouque, Xinyong Liu

PII: S0968-0896(14)00135-7
DOI: http://dx.doi.org/10.1016/j.bmc.2014.02.029
Reference: BMC 11418

To appear in: *Bioorganic & Medicinal Chemistry*

Received Date: 15 December 2013
Revised Date: 18 February 2014
Accepted Date: 22 February 2014

Please cite this article as: Tian, Y., Du, D., Rai, D., Wang, L., Liu, H., Zhan, P., De Clercq, E., Pannecouque, C., Liu, X., Fused heterocyclic compounds bearing bridgehead nitrogen as potent HIV-1 NNRTIs. Part 1: Design, synthesis and biological evaluation of novel 5,7-disubstituted pyrazolo[1,5-*a*]pyrimidine derivatives, *Bioorganic & Medicinal Chemistry* (2014), doi: http://dx.doi.org/10.1016/j.bmc.2014.02.029

Fused heterocyclic compounds bearing bridgehead nitrogen as potent HIV-1 NNRTIs. Part 1: Design, synthesis and biological evaluation of novel 5,7-disubstituted pyrazolo[1,5-*a*]pyrimidine derivatives

Ye Tian[1], Deping Du[1], Diwakar Rai[1], Liu Wang[1], Huiqing Liu[2], Peng Zhan[1,*], Erik De Clercq[3], Christophe Pannecouque[3], Xinyong Liu[1,*]

[1] Department of medicinal Chemistry, Key Laboratory of Chemical Biology (Educational Ministry of China), School of Pharmaceutical Sciences, Shandong University, No.44 Wenhuaxi Road, Jinan 250012, China

[2] Institute of Pharmacology, School of Medicine, Shandong University, 44, West Culture Road, 250012 Jinan, Shandong, PR China

[3] Rega Institute for Medical Research, KU Leuven, Minderbroedersstraat 10, B-3000 Leuven, Belgium

*Phone: +86-531-88380270. Fax: +86-531-88382731. E-mail: zhanpeng1982@sdu.edu.cn (Zhan P.); xinyongl@sdu.edu.cn (Liu X.Y.).

Abstract

In our continuous efforts to identify novel potent HIV-1 NNRTIs, a novel class of 5,7-disubstituted pyrazolo[1,5-*a*]pyrimidine derivatives were rationally designed, synthesized and evaluated for their anti-HIV activities in MT4 cell cultures. Biological results showed that most of the tested compounds displayed excellent activity against wild-type HIV-1 with a wide range of EC_{50} values from 5.98 μM to 0.07 μM. Among the active compounds, **5a** was found to be the most promising analogue with an EC_{50} of 0.07 μM against wild-type HIV-1 and very high selectivity index (SI, 3999). Compound **5a** was more effective than the reference drugs nevirapine (by 2-fold) and delavirdine (by 2-fold). In order to further confirm their binding target, an HIV-1 RT inhibitory assay was also performed. Furthermore, SAR analysis among the newly synthesized compounds was discussed and the binding mode of the active compound **5a** was rationalized by molecular modelling studies.

Key words HIV-1, RT, NNRTIs, heterocycle, pyrazolo[1,5-*a*]pyrimidine, synthesis, activity assay, molecular modeling.

1. Introduction

Up to now, five HIV-1 non-nucleoside reverse transcriptase inhibitors (NNRTIs) have already been launched on the market and are widely used for the treatment of AIDS as one important component of highly active antiretroviral therapy (HAART). However, the usage of existing drugs, especially the first generation NNRTIs (nevirapine, delavirdine and efavirenz), has been compromised by the emergence of drug-resistant viral strains which have common mutants in the binding pocket of RT [1]. This has driven medicinal chemists to further develop novel NNRTIs with high potency and improved anti-resistance profiles.

Diarylpyrimidine (DAPY) analogues was proved to be one of the most important and promising class of HIV-1 NNRTIs. As the second-generation NNRTIs, DAPYs demonstrate extremely excellent potency against both the wild-type (WT) virus and

mutant strains [2-5]. So far, two drugs belonging to this series TMC125 (etravirine, ETV) and TMC278 (rilpivirine), have been approved by FDA [6] (**Fig. 1**). Over the past few years, considerable efforts have been devoted to the structural modification of DAPYs, leading to the discovery of highly potent drug candidates. Recently, pyrrolopyrimidine derivatives RDEA427 and RDEA640 have been disclosed [7-9] to possess excellent HIV antiviral activity against wild-type (with EC_{50} values of 0.9 nM and 0.8 nM, respectively) and a broad panel of NNRTI-resistant mutant viruses (e.g., the fold-changes in EC_{50} against K103N-Y181C mutant strains was 11 and 3.8, respectively) with low potential for human cytochrome P450 (CYP) induction and large selectivity index (SI > 50,000). It is worth noting that RDEA427 has better metabolic stability and lower covalent binding potential than RDEA640 or TMC278 and is undergoing preliminary clinical evaluation (**Fig.1**).

Figure 1. Representative analogues of the DAPY series.

As part of our research interest on these DAPY-like NNRTIs [10-13], encouraged by the promising results of pyrrolopyrimidine derivatives, we conducted molecular modifications by core refinements and substituents' optimization for obtaining improved anti-HIV activity and pharmacokinetic profiles (**Fig. 2**). According to the bioisosterism of drug design, we employed the bridgehead nitrogen heterocycle pyrazolo[1,5-*a*]pyrimidine as the central ring and adopted various groups of two 'wings' of the molecule in order to explore the steric, electrical and hydrophobic effects of the nucleus and substituents, while keeping the overall molecular conformation of DAPYs which is required for the anti-RT potency. To achieve our goal, novel 5,7-disubstituted pyrazolo[1,5-*a*]pyrimidine derivatives were designed, synthesized and evaluated for their anti-HIV activities in cell line and enzyme inhibition.

Figure 2. Structure-based biosterism design of 5,7-disubstituted pyrazolo[1,5-*a*]pyrimidine derivatives as HIV-1 NNRTIs.

2. Results and Discussion

2.1 Chemistry

The synthetic route of target compounds pyrazolo[1,5-*a*]pyrimidine derivatives is depicted in **Scheme 1**.

Scheme 1. The synthetic route for pyrazolo[1,5-*a*]pyrimidine derivatives. **Reagents and conditions**: (i) Diethyl malonate, Na, EtOH; (ii) $POCl_3$, Dimethylaniline; (iii) ArOH, K_2CO_3, DMF; (iv) ArOH, $Pd(OAc)_2$, Xantphos, Cs_2CO_3, 1,4-Dioxane

For the preparation of the designed series, commercially available 1*H*-pyrazol-5-amine (**1**) was used as the starting material that reacted with diethyl malonate to form the pyrazolo[1,5-*a*]pyrimidine system (**2**). Chlorination of **2** with $POCl_3$ afforded the key intermediate 5,7-dichloropyrazolo[1,5-*a*]pyrimidine (**3**) by the reported method [14]. Then different phenols were connected to the relatively active 7-position [15, 16] of the fused pyrazolo[1,5-*a*]pyrimidine ring by a nucleophilic aromatic substitution reaction under mild reaction condition, providing intermediates **4**-**9**. At last, in the presence of $Pd(OAc)_2$ and Xantphos catalytic system (Buchwald-Hartwig reaction), **4**-**9** were reacted with various anilines and yielded 18 title compounds (**4a-g**, **5a-g**, **6a**, **7a**, **8a**, **9a**). The synthesized compounds were characterized by physicochemical and spectral means and the IR, MS, ^{1}H-NMR, ^{13}C-NMR spectral data were found in agreement with the assigned molecular structures.

2.2 Anti-HIV-1 (IIIB) activity

All the synthesized compounds were evaluated for their antiviral activity based on their capacity to inhibit the replication of wild-type HIV-1 (III_B), mutated HIV-1 (RES056) and HIV-2 (ROD) strains in MT4 cell cultures, using the MTT assay. The FDA approved drugs nevirapine (NVP) and delavirdine (DLV) were used as controls. The reported activity of etravirine (ETV) was also included as reference standard. The bioactivity results of 18 compounds are presented in **Table 1**.

It is worth noting that, except for compound **8a**, all the newly synthesized compounds demonstrated moderate to excellent anti-HIV-1 activity with EC_{50} ranging from 5.98 μM to 0.07 μM, while none of them were active against HIV-2. Among them, compound **5a** was identified as the most active derivative against wild-type HIV-1 (EC_{50} = 0.07 μM and SI of 3,999). In comparison with the reference drugs, compound **5a** was two-fold more potent than NVP and DLV against HIV-1 III_B strain, but was still inferior to the clinically used etravirine (3nM) (as a reference here, the data were obtained from the same lab of the Rega Institute for Medical Research, KU Leuven, Belgium) [17]. Besides, other three compounds (**5b**, EC_{50} = 0.14 μM; **5c**, EC_{50} = 0.17 μM; **5e**, EC_{50} = 0.17 μM) also showed better or comparable potency than the control drugs (**NVP**, EC_{50} = 0.17 μM; **DLV**, EC_{50} = 0.16 μM). Although these pyrazolo[1,5-*a*]pyrimidines did not provide the improved activity in comparison with ETV, they represent a novel class of antiviral agents with great potential for further investigation. Preliminary structure-activity relationship (SAR) derived from these results was analyzed as follows.

First of all, the nature of the 4-substitutions of anilines connecting to the right wing was investigated by introducing a series of different groups in this site while keeping other positions unchanged. In the **4a-g** subseries with a 2,6-dimethyl-4-cyano substituent in the left wing, compounds **4a** (-CN) and **4b** (-Br) showed similar potency, while the presence of chloride atom slightly increased the activity (**4c**). The introduction of a methoxyl group afforded **4f** with further improved EC_{50} value of 0.91 μM, and the **4e** bearing 4-methyl substituent displayed the best activity (EC_{50} = 0.46 μM) in this subseries, whereas the F- or NO_2- obviously decreased their effectiveness against HIV-1. On the whole, the effect of diverse functional groups of **5a-g** on anti-HIV-1 activity is similar to that of **4a**-**g**, but there are also some differences. Compound **5a** was found to be the most promising compound with the lowest EC_{50} and the highest selective index (SI = 3,999) of this series. The data suggested that the substitution on the right ring played a significant role in the antiviral activity profiles.

To illuminate the SAR of the left wing, the EC_{50} values of compounds **4a**, **5a**, **6a**,

7a, **8a** and **9a** were compared, which suggested the *para*-substituent of phenol was pivatal for the anti-HIV-1 potency. We found that compounds **5a-g** with the 2,4,6-trimethyl substituent exhibited 3~20-fold better potency than their corresponding analogues in **4a**-**g**, which suggested the more favorable property of 2,4,6-trimetyl substituent than 2,6-dimethyl-4-cyano of the left phenol of these molecule. Besides, **7a** (trifluoro-) and **9a** (3,5-dimethyl) have only moderate activity, and **8a** totally lost the activity with the SI < 1. So, the order of other substituents based on the potency was: 2,4,6-trimethyl (**5a**) > 2,6-dimethyl-4-bromo (**6a**) > 2,6-dimethyl-4-cyano (**4a**) > 3,5-dimethyl (**9a**) > trifluoro (**7a**).

Unfortunately, the bioactivity results also demonstrated that all the title compounds were inactive against mutated HIV-1 strain RES056 bearing both the K103N and Y181C mutations.

Regarding to the cytotoxicity, compounds bearing various substituents were roughly ranked in the following sequence: MeO < NO_2 < CN ≈F < Me ≈ Cl < Br (substituents on the right aniline); 2,4,6-trimethyl < 2,6-dimethyl-4-bromo < 3,5-dimethyl ≈ 2,6-dimethyl < 2,6-dimethyl-4-cyano (substituents on left phenol). Among them, compound **4b** exhibited the greatest toxicity with an CC_{50} of 8.51 μM while **5f** was the least toxic one with a CC_{50} higher than 334 μM.

Table 1. Inhibitory action of compounds **4a-g**, **5a-g**, **6a**, **7a**, **8a**, **9a** against HIV replication and cytotoxicity in MT-4 cells.

2.3 HIV-RT inhibitory activity evaluation

To further characterize the mechanism of action of the newly designed compounds, the most active **5a** as a representative compound was chosen to evaluate the HIV-RT inhibitory activity using the HIV-RT kit assay, together with the marketed drugs of NVP and ETV as the controls [18]. As listed in **Table 2**, the data revealed that compound **5a** exhibited its inhibitory activity with an IC_{50} value of 2.25 μM, which is about 5 times and 28 times lower than that of reference drug NVP (IC_{50} = 0.55 μM) and ETV (IC_{50} = 0.08 μM), respectively. The results seemed to indicate that this type of 5,7-disubstitutedpyrazolo[1,5-*a*]pyrimidine derivatives acted as HIV-1 NNRTIs. However, the inhibitory activity against HIV-RT did not correspond to the anti-HIV efficiency in the MTT cell assay, which is probably due to the physicochemical properties (e.g., membrane permeability) or target promiscuity (potential to bind to other targets) of the tested compounds demonstrating different impact on the cellular and enzymatic assays.

Table 2. Activity of pyrazolo[1,5-*a*]pyrimidine derivative **5a** against HIV-1 RT.

2.4 Molecular modeling study

To understand the binding mode of these novel pyrazolo[1,5-*a*]pyrimidine derivatives, a docking study was performed using the Surflex-Dock module of Sybyl-X 1.1 software. The most active molecule **5a** was chosen as a representative to be docked into the non-nucleoside binding site (NNBS) of HIV-1 RT (taken from the crystal structure of RT/TMC125, PDB code: 3MEC). And the lead compounds TMC125 and RDEA640 were also studied as references. Surflex-Dock GeomX (SFXC) mode was applied and the obtained scores are shown in **Table 3**. All three compounds have excellent total scores. Most of these figures of the tested compound **5a** and two reference molecules are very similar, while the absolute value of the

'Crash' item of **5a** is significantly larger than these of the others. This indicated that an inappropriate targeting of **5a** with the protein might explain why **5a** demonstrated relatively lower anti-HIV-1 activity. Additionally, the binding mode analysis suggested that compound **5a** binds to HIV-1 RT in an U-shape and shares a close similar conformation with TMC125 and RDEA640 (**Fig. 3a**). Their resulting structures can overlap very well including the original ligand contained in the crystal. According to the mode of action (**Fig. 3b**), the N atom at 4 position of the fused ring and the NH group linked to the 5-position of the core could make hydrogen bonds with Lys101. Further, the mesityloxy of **5a** points to the aromatic-rich binding pocket surrounded by the aromatic Tyr181, Tyr188, Phe227 and Trp229 through π–π interactions, while the 4-cyanoaniline ring parallels the Tyr318 position. However, the lack of one polar interaction between the pyrazole part of **5a** and Glu138 may be another reason for the inferior potency of **5a**. The computational modeling study has helped in understanding the interactions between these inhibitors and the HIV-1 RT.

Table 3. Docking scores[a] of TMC125, RDEA640 and **5a** by Surflex-Dock.

(a) (b)

Figure 3. Docking of **5a** is shown by Pymol (version: 0.99rc6): (a) Molecular superposition of **5a** (carbon atoms in yellow) with TMC125 (original ligand extracted from 3MEC, carbon atoms in gray; newly docked molecule as the reference, carbon atoms in pink) and RDEA640 (carbon atoms in salmon) in the binding site; (b) Molecular model of **5a** in the RT non-nucleoside binding site (PDB code: 3MEC).

2.5 Physicochemical Properties study

Furthermore, the physicochemical properties (logP, molecular weight, topological polar surface area, molecular volume etc.) of **5a** (as representative structures), ETV and NVP (as control) were determined using free on-line molinspiration software (*http://www.molinspiration.com/*) for their compliance to the Lipinski's rule of five [19]. The physicochemical results (**Table 4**) suggested that

compounds **5a**, nevirapine and TMC125 agreed well with the Lipinski's rule of five. Additionally, pyrazolo[1,5-*a*]pyrimidine derivatives and ETV share very similar properties. Their physicochemical properties would not be mainly responsible for their moderate activity against HIV-1.

Table 4. Physicochemical properties[a] of **5a**, ETV and NVP.

3. Conclusion

In brief, based on the bioisosterism and core refinements strategies of drug design, with convenient and efficient synthesis, biological evaluation, a novel series of 5,7-disubstituted pyrazolo[1,5-*a*]pyrimidine derivatives was identified as potent HIV-1 inhibitors. Most of these compounds exhibited good activity against HIV-1 with EC_{50} values ranging from 70 nM to micromolar concentrations. Among them, compound **5a** was identified as the most promising candidate in inhibiting HIV-1 replication with EC_{50} value of 0.070 μM and the SI of 3,999, which were much better than those of NVP (EC_{50} = 0.17 μM) and DLV (EC_{50} = 0.16 μM). Although compound **5a** was less active than ETV, these promising results demonstrated that the isosteric replacement of pyrazolo[1,5-*a*]pyrimidine for pyrimidine in the central ring of DAPY compounds was gratifying and afforded a series of potent bridgehead nitrogen heterocycle-derived NNRTIs. Further, preliminary SAR information has been summarized. The results of in vitro HIV-RT kit assay and docking study for compound **5a** indicates its possible mechanisms of action. These valuable information and readily accessible synthetic methods greatly encourage us to further optimize the promising structures, which will be reported in due course.

4. Materials and Methods

4.1 Chemistry

All melting points (mp) were determined on a micromelting point apparatus and are uncorrected. Mass spectra were taken on a LC Autosampler Device: Standard G1313A instrument by electrospray ionization. ^{1}H-NMR spectra were obtained on a

Brucker Avance-400 NMR-spectrometer in the indicated solvents. Chemical shifts are reported in δ units and TMS as an internal reference. The ^{13}C-NMR spectra were recorded on a Brucker Avance-100 NMR-spectrometer and are reported accordingly. TLC was performed on Silica Gel GF254 for TLC and spots were visualized by irradiation with UV light (254 nm). Flash column chromatography was performed on a column packed with Silica Gel 60 (200-300 mesh). Solvents were reagent grade and, when necessary, were purified and dried by standard methods. Concentration of the reaction solution involved the use of rotary evaporator at reduced pressure.

4.2 General synthetic procedure for compounds 5-chloro-7-subtitutedphenoxypyrazolo[1,5-*a*]pyrimidines (4-9)

3-Aminopyrazole **(1)** (20 mmol, 1 eq) and diethyl malonate (22 mmol, 1.1 eq) were added to a freshly made solution of sodium metal (40 mmol, 2 eq) in ethanol (60 mL). The mixture was heated to 80 °C and stirred for 5 hours. After the reaction, the solution was cooled to room temperature and filtered. The obtained solid was washed with ethanol and dissolved in water (30 mL). Then the solution was acidified to pH 1~2 using concentrated HCl in an ice-bath. The precipitate was filtered, washed with water and dried to give light yellow powder (**2**, yield 73.2%, EI-MS: 152.2 [M+H], 174.3 [M+Na]) that was directly used in next step.

Pyrazolo[1,5-*a*]pyrimidine-5,7(4*H*,6*H*)-dione (**2**) (20 mmol, 1 eq) was added to the mixture of $POCl_3$ (440 mmol, 22 eq) and dimethylaniline (60 mmol, 3 eq) in an ice-bath under nitrogen protection. The solution was stirred overnight at 80 °C and then cooled and concentrated. The obtained residue was dissolved in methylene chloride (50 mL) and poured into ice-water. After being stirred for 10 min, it was adjusted to pH 8~9 using solid $NaHCO_3$. The organic layer was then separated, washed (water), dried ($MgSO_4$), filtered and concentrated. The crude product was purified by flash chromatographic column to afford 5,7-dichloropyrazolo[1,5-*a*]pyrimidine (**3**) with a yield of 61.2% (EI-MS: 188.3 [M+H], 190.4 [M+H]).

5,7-Dichloropyrazolo[1,5-*a*]pyrimidine (**3**, 2.5 mmol, 1 eq) and appropriate

substituted phenol (2.5 mmol, 1 eq) and potassium carbonate (5mmol, 2 eq) were added to DMF, and then stirred for 12 hours at room temperature. After the reaction was ended, water was added to the mixture to give more precipitate. The crude product 5-chloro-7-subtitutedphenoxypyrazolo[1,5-*a*]pyrimidine (**4-9**) was obtained by filtration and desiccation with good yield (**4**: yield 98.1%, EI-MS: 299.4 [M+H], 301.3 [M+H]; **5**: yield 99.5%, EI-MS: 288.2 [M+H], 290.3 [M+H]; **6**: yield 96.9%, EI-MS: 352.2 [M+H], 354.1 [M+H]; **7**: yield 93.6%, EI-MS: 300.3 [M+H], 302.3 [M+H]; **8**: yield 89.6%, EI-MS: 274.3 [M+H], 276.4 [M+H]; **9**: yield 96.5%, EI-MS: 274.3 [M+H], 276.3 [M+H]).

4.3 General synthetic procedure for target compounds (4a-g, 5a-g, 6a, 7a, 8a, 9a)

$Pd(OAc)_2$ (0.025 mmol, 0.05 eq) and Xantphos (0.05 mmol, 0.1 eq) were added to 1,4-dioxane (3 mL), after stirring for 15 min at room temperature, 5-chloro-7-subtitutedphenoxypyrazolo[1,5-*a*]pyrimidine (0.5 mmol, 1 eq) (**4-9**), 4-substitued aniline (0.6 mmol, 1.2 eq) and Cs_2CO_3 (0.75 mmol, 1.5 eq), were added to the mixture. The reaction mixture was allowed to stir overnight at 100 °C under N_2 protection, and then the solution was cooled and concentrated. Further, water (20 mL) and CH_2Cl_2 (20 mL) were added to the residue for extraction, the obtained organic phase was dried ($MgSO_4$), filtered and concentrated under reduced pressure. Flash chromatography and recrystallization using proper solvent finally give the pyrazolo[1,5-*a*]pyrimidine derivatives (**4a-g**, **5a-g**, **6a**, **7a**, **8a**, **9a**).

4-(5-(4-cyanophenylamino)pyrazolo[1,5-*a*]pyrimidin-7-yloxy)-3,5-dimethylbenzonitrile (4a)

White crystal, yield: 22.6%. Mp: > 300°C; ^{1}H-NMR (DMSO-d_6) δppm: 2.22 (s, 6H, CH_3), 5.49 (s, 1H, -CH=), 6.42 (d, 1H, J = 2.1 Hz, -CH=), 7.74-7.94 (m, 4H, benzene), 7.91 (s, 2H, benzene), 8.10 (d, 1H, J = 2.1 Hz, -CH=), 9.81 (s, 1H, NH); ^{13}C-NMR (DMSO-d_6) δppm: 15.56 (-CH_3 ×2), 118.60 (-CN), 119.90 (-CN), Ar-C (×18): 80.37, 94.54, 103.40, 110.47, 118.74, 133.03 (×2), 133.71 (×2), 134.07 (×2), 145.67, 145.67, 149.62, 152.08, 152.64, 154.19; EI-MS: 381.4 [M+H], 403.4

[M+Na].

4-(5-(4-bromophenylamino)pyrazolo[1,5-*a*]pyrimidin-7-yloxy)-3,5-dimethylbenzonitrile (4b)

White crystal, yield: 52.9%. Mp: > 300°C; ^{1}H-NMR (DMSO-d_6) δppm: 2.22 (s, 6H, CH_3), 5.42 (s, 1H, -CH=), 6.32 (d, 1H, *J* = 2.1 Hz, -CH=), 7.46-7.73 (m, 4H, benzene), 7. 89 (s, 2H, benzene), 8.04 (d, 1H, *J* = 2.1 Hz, -CH=), 9.45 (s, 1H, NH); ^{13}C-NMR (DMSO-d_6) δppm: 15.56 (-CH_3 ×2), 118.59 (-CN), Ar-C (×18): 80.07, 93.95, 110.42, 113.66, 120.49 (×2), 131.91 (×2),133.02 (×2), 134.01 (×2), 140.16, 145.42, 149.95, 152.19, 152.44, 154.50; EI-MS: 434.3 [M+H], 436.3 [M+H].

4-(5-(4-chlorophenylamino)pyrazolo[1,5-*a*]pyrimidin-7-yloxy)-3,5-dimethylbenzonitrile (4c)

White crystal, yield: 63.2%. Mp: 285-287°C; ^{1}H-NMR (DMSO-d_6) δppm: 2.22 (s, 6H, CH_3), 5.42 (s, 1H, -CH=), 6.32 (d, 1H, *J* = 2.1 Hz, -CH=), 7.34-7.78 (m, 4H, benzene), 7. 89 (s, 2H, benzene), 8.04 (d, 1H, *J* = 2.1 Hz, -CH=), 9.45 (s, 1H, NH); ^{13}C-NMR (DMSO-d_6) δppm: 15.56 (-CH_3 ×2), 118.61 (-CN), Ar-C (×18): 80.00, 93.94, 110.40, 120.46 (×2), 125.73, 129.04 (×2), 133.02 (×2), 134.03 (×2), 139.75, 145.42, 149.93, 152.16, 152.41, 154.50; EI-MS: 390.3 [M+H], 392.3 [M+H].

4-(5-(4-fluorophenylamino)pyrazolo[1,5-*a*]pyrimidin-7-yloxy)-3,5-dimethylbenzonitrile (4d)

White powder, yield: 59.0%. Mp: 251-252°C; ^{1}H-NMR (DMSO-d_6) δppm: 2.22 (s, 6H, CH_3), 5.40 (s, 1H, -CH=), 6.28 (d, 1H, *J* = 2.1 Hz, -CH=), 7.12-7.76 (m, 4H, benzene), 7.89 (s, 2H, benzene), 8.02 (d, 1H, *J* = 2.1 Hz, -CH=), 9.34 (s, 1H, NH); ^{13}C-NMR (DMSO-d_6) δppm: 15.57 (-CH_3 ×2), 118.62 (-CN), Ar-C (×18): 79.80, 93.72, 110.37, 115.61, 115.83, 120.73 (×2), 133.02 (×2), 134.02 (×2), 137.18 (×2), 145.37, 150.05, 152.19 (×2), 154.64; EI-MS: 374.3 [M+H].

4-(5-(4-methylphenylamino)pyrazolo[1,5-*a*]pyrimidin-7-yloxy)-3,5-dimethylbenzonitrile (4e)

Light orange crystal, yield: 31.2%. Mp: 280-282°C; ^{1}H-NMR (DMSO-d_6) δppm: 2.22 (s, 6H, CH_3), 2.24 (s, 3H, CH_3), 5.41 (s, 1H, -CH=), 6.26 (d, 1H, *J* = 2.1 Hz, -CH=), 7.09-7.62 (m, 6H, benzene), 7. 89 (s, 2H, benzene), 8.00 (d, 1H, *J* = 2.1 Hz,

-CH=), 9.21 (s, 1H, NH); ^{13}C-NMR (DMSO-d_6) δppm: 15.56 (-CH_3 ×2), 20.87 (-CH_3), 110.34 (-CN), Ar-C (×18): 93.55, 118.61, 119.22 (×2), 129.56 (×3), 131.24, 133.02 (×2), 133.99 (×2), 138.25, 145.25, 150.22, 152.25 (×2), 154.77; EI-MS: 368.3 [M-H].

4-(5-(4-methoxyphenylamino)pyrazolo[1,5-*a*]pyrimidin-7-yloxy)-3,5-dimethylbenzonitrile (4f)

White powder, yield: 19.3%. Mp: > 300°C; ^{1}H-NMR (DMSO-d_6) δppm: 2.22 (s, 6H, CH_3), 3.72 (s, 3H, CH_3), 5.36 (s, 1H, -CH=), 6.22 (d, 1H, *J* = 2.1 Hz, -CH=), 6.87-7.62 (m, 4H, benzene), 7. 89 (s, 2H, benzene), 7.98 (d, 1H, *J* = 2.1 Hz, -CH=), 9.14 (s, 1H, NH); ^{13}C-NMR (DMSO-d_6) δppm: 15.57 (-CH_3 ×2), 55.65 (-CH_3), 118.78 (-CN), Ar-C (×18): 79.71, 93.36, 110.32, 114.40 (×2), 120.86 (×2), 133.02 (×2), 133.98 (×3), 145.19 150.30, 152.26 (×2), 154.80 (×2); EI-MS: 386.4 [M+H], 408.4 [M+Na].

4-(5-(4-nitrophenylamino)pyrazolo[1,5-*a*]pyrimidin-7-yloxy)-3,5-dimethylbenzonitrile (4g)

Greenyellow crystal, yield: 37.3%. Mp: > 300°C; ^{1}H-NMR (DMSO-d_6) δppm: 2.23 (s, 6H, CH_3), 5.53 (s, 1H, -CH=), 6.45 (d, 1H, *J* = 2.1 Hz, -CH=), 7.91 (s, 2H, benzene), 7.96-8.24 (m, 4H, benzene), 8.13 (d, 1H, *J* = 2.1 Hz, -CH=), 10.02 (s, 1H, NH); ^{13}C-NMR (DMSO-d_6) δppm: 15.56 (-CH_3 ×2), 118.58 (-CN), Ar-C (×18): 80.55, 94.75, 110.51, 118.21 (×2), 125.64 (×2), 133.03 (×2), 134.07 (×2), 141.17, 145.77, 147.08, 149.52, 152.08, 152.74, 154.00; EI-MS: 401.4 [M+H], 423.4 [M+Na].

4-(7-(mesityloxy)pyrazolo[1,5-*a*]pyrimidin-5-ylamino)benzonitrile (5a)

Cream white crystal, yield: 28.1%. Mp: > 300°C; ^{1}H-NMR (DMSO-d_6) δppm: 2.12(s, 6H, CH_3), 2.32(s, 3H, CH_3), 5.50 (s, 1H, -CH=), 6.39 (d, 1H, *J* = 2.1 Hz, -CH=), 7.11 (s, 2H, benzene), 7.73-7.95 (m, 4H, benzene), 8.08 (d, 1H, *J* = 2.1 Hz, -CH=), 9.83 (s, 1H, NH); ^{13}C-NMR (DMSO-d_6) δppm: 15.71 (-CH_3 ×2), 20.82 (-CH_3), 119.91 (-CN), Ar-C(×18): 79.95, 94.28, 103.27, 118.74 (×2), 130.12 (×2), 130.57 (×2), 133.62 (×2), 136.71, 145.16, 145.42, 146.50, 149.61, 153.83, 154.45; EI-MS: 370.4 [M+H], 392.4 [M+Na].

N-(4-bromophenyl)-7-(mesityloxy)pyrazolo[1,5-*a*]pyrimidin-5-amine (5b)

Light yellow crystal, yield: 49.2%. Mp: 286-287°C; ^{1}H-NMR (DMSO-d_6) δppm:

2.12(s, 6H, CH_3), 2.32(s, 3H, CH_3), 5.42 (s, 1H, -CH=), 6.29 (d, 1H, *J* = 2.1 Hz, -CH=), 7.10 (s, 2H, benzene), 7.44-7.74 (m, 4H, benzene), 8.01 (d, 1H, *J* = 2.1 Hz, -CH=), 9.47 (s, 1H, NH); ^{13}C-NMR (DMSO-d_6) δppm: 15.74 (-CH_3 ×2), 20.84 (-CH_3), Ar-C(×18): 79.56, 93.75, 113.46, 120.83 (×2), 130.12 (×2), 130.54 (×2), 131.87 (×2), 136.62, 140.33, 145.18, 146.49, 149.87, 153.54, 154.73; EI-MS: 423.3 [M+H], 425.3 [M+H].

N-(4-chlorophenyl)-7-(mesityloxy)pyrazolo[1,5-*a*]pyrimidin-5-amine (5c)

White crystal, yield: 40.6%. Mp: 274-275°C; ^{1}H-NMR (DMSO-d_6) δppm: 2.12(s, 6H, CH_3), 2.32(s, 3H, CH_3), 5.43 (s, 1H, -CH=), 6.29 (d, 1H, *J* = 2.1 Hz, -CH=), 7.10 (s, 2H, benzene), 7.32-7.80 (m, 4H, benzene), 8.02 (d, 1H, *J* = 2.1 Hz, -CH=), 9.47 (s, 1H, NH); ^{13}C-NMR (DMSO-d_6) δppm: 15.73 (-CH_3 ×2), 20.83 (-CH_3), Ar-C(×18): 79.54, 93.71, 120.42 (×2), 125.55, 128.98 (×2), 130.12 (×2), 131.54 (×2), 136.62, 139.93, 145.17, 146.50, 149.89, 153.55, 154.75; EI-MS: 379.4 [M+H], 381.4 [M+H].

N-(4-fluorophenyl)-7-(mesityloxy)pyrazolo[1,5-*a*]pyrimidin-5-amine (5d)

White crystal, yield: 32.4%. Mp: 252-253°C; ^{1}H-NMR (DMSO-d_6) δppm: 2.13(s, 6H, CH_3), 2.32(s, 3H, CH_3), 5.40 (s, 1H, -CH=), 6.25 (d, 1H, *J* = 2.1 Hz, -CH=), 7.10-7.77 (m, 6H, benzene), 8.00 (d, 1H, *J* = 2.1 Hz, -CH=), 9.37 (s, 1H, NH); ^{13}C-NMR (DMSO-d_6) δppm: 15.74 (-CH_3 ×2), 20.83 (-CH_3), Ar-C (×18): 79.33, 93.49, 115.54, 115.76, 120.59, 120.66, 130.12 (×2), 130.53 (×2), 136.59, 145.08, 146.51, 150.01, 153.46, 154.88, 156.44, 158.80; EI-MS: 363.4 [M+H], 385.4 [M+Na].

7-(mesityloxy)-N-*p*-tolylpyrazolo[1,5-*a*]pyrimidin-5-amine (5e)

Cream white crystal, yield: 41.3%. Mp: 251-253°C; ^{1}H-NMR (DMSO-d_6) δppm: 2.12 (s, 6H, CH_3), 2.24 (s, 3H, CH_3), 2.32 (s, 3H, CH_3), 5.41 (s, 1H, -CH=), 6.23 (d, 1H, *J* = 2.1 Hz, -CH=), 7.09 (s, 2H, benzene), 7.07-7.62 (m, 4H, benzene), 7.97 (d, 1H, *J* = 2.1 Hz, -CH=), 9.24 (s, 1H, NH); ^{13}C-NMR (DMSO-d_6) δppm: 15.75 (-CH_3 ×2), 20.84 (-CH_3), 20.88 (-CH_3), Ar-C (×18): 79.42, 93.35, 119.15 (×2), 129.51 (×2), 130.13 (×2), 130.51 (×2), 131.02, 136.53, 138.43, 145.00, 146.54, 150.16, 153.35, 155.01; EI-MS: 359.4 [M+H], 381.4 [M+Na].

7-(mesityloxy)-N-(4-methoxyphenyl)pyrazolo[1,5-*a*]pyrimidin-5-amine (5f)

White crystal, yield: 29.2%. Mp: 213-215°C; ^{1}H-NMR (DMSO-d_6) δppm: 2.12 (s, 6H, CH_3), 2.31 (s, 3H, CH_3), 3.71 (s, 3H, CH_3), 5.36 (s, 1H, -CH=), 6.19 (d, 1H, J = 2.1 Hz, -CH=), 7.09 (s, 2H, benzene), 6.86-7.63 (m, 4H, benzene), 7.96 (d, 1H, J = 2.1 Hz, -CH=), 9.17 (s, 1H, NH); ^{13}C-NMR (DMSO-d_6) δppm: 15.75 (-CH_3 ×2), 20.84 (-CH_3), 55.62 (-CH_3), Ar-C (×18): 79.21, 93.14, 114.33 (×2), 120.76 (×2), 130.13 (×2), 130.50 (×2), 134.10, 136.51, 144.94, 146.54, 150.24, 153.30, 154.81, 155.04; EI-MS: 375.4 [M+H].

7-(mesityloxy)-N-(4-nitrophenyl)pyrazolo[1,5-*a*]pyrimidin-5-amine (5g)

Yellow needle crystal, yield: 33.4%. Mp: 283-284°C; ^{1}H-NMR (DMSO-d_6) δppm: 2.13(s, 6H, CH_3), 2.33(s, 3H, CH_3), 5.54 (s, 1H, -CH=), 6.42 (d, 1H, J = 2.1 Hz, -CH=), 7. 12 (s, 2H, benzene), 8.10 (d, 1H, J = 2.1 Hz, -CH=), 7.97-8.22 (m, 4H, benzene), 9.37 (s, 1H, NH); ^{13}C-NMR (DMSO-d_6) δppm: 15.71 (-CH_3 ×2), 20.83 (-CH_3), Ar-C(×18): 80.12, 94.50, 118.18 (×2), 125.57 (×2), 130.12 (×2), 130.58 (×2), 136.75, 141.04, 145.53, 146.49, 147.28, 149.50, 153.93, 154.24; EI-MS: 390.3 [M+H], 412.4 [M+Na].

4-(7-(4-bromo-2,6-dimethylphenoxy)pyrazolo[1,5-*a*]pyrimidin-5-ylamino)benzonitrile (6a)

White crystal, yield: 43.9%. Mp: > 300°C; ^{1}H-NMR (DMSO-d_6) δppm: 2.17(s, 6H, CH_3), 5.52 (s, 1H, -CH=), 6.41 (d, 1H, J = 2.1 Hz, -CH=), 7. 58 (s, 2H, benzene), 7.74-7.95 (m, 4H, benzene), 8.09 (d, 1H, J = 2.1 Hz, -CH=), 9.81 (s, 1H, NH); ^{13}C-NMR (DMSO-d_6) δppm: 15.55 (-CH_3 ×2), 119.91 (-CN), Ar-C(×18): 80.13, 94.42, 103.33, 118.71 (×2), 119.87, 132.55 (×2), 133.47 (×2), 133.68 (×2), 145.05, 145.55, 147.94, 149.62, 153.19, 154.32; EI-MS: 434.4 [M+H], 436.4 [M+H].

4-(7-(2,4,6-trifluorophenoxy)pyrazolo[1,5-*a*]pyrimidin-5-ylamino)benzonitrile (7a)

Pink crystal, yield: 43.5%. Mp: 247-250°C; ^{1}H-NMR (DMSO-d_6) δppm: 5.88 (s, 1H, -CH=), 6.45 (d, 1H, J = 2.1 Hz, -CH=), 7.73 (t, 2H, benzene, J = 8.7 Hz), 7.77-7.96 (m, 4H, benzene), 8.13 (d, 1H, J = 2.1 Hz, -CH=), 9.90 (s, 1H, NH); ^{13}C-NMR (DMSO-d_6) δppm: 119.81 (-CN), Ar-C(×18): 80.64, 94.64, 103.04, 103.28, 103.55, 103.74, 118.95 (×3), 133.70 (×3), 144.77, 145.95, 149.68, 153.43, 153.98;

EI-MS: 382.4 [M+H], 404.4 [M+Na].

4-(7-(2,6-dimethylphenoxy)pyrazolo[1,5-*a*]pyrimidin-5-ylamino)benzonitrile (8a)

White crystal, yield: 15.7%. Mp: 270-273°C; ^{1}H-NMR (DMSO-d_6) δppm: 2.35(s, 6H, CH_3), 5.64 (s, 1H, -CH=), 6.38 (d, 1H, J = 2.1 Hz, -CH=), 7. 09 (s, 3H, benzene), 7.73-7.96 (m, 4H, benzene), 8.05 (d, 1H, J = 2.1 Hz, -CH=), 9.87 (s, 1H, NH); ^{13}C-NMR (DMSO-d_6) δppm: 21.26 (-CH_3 ×2), 119.91 (-CN), Ar-C(×18): 81.54, 94.24, 103.29, 118.78 (×2), 119.04 (×2), 128.95, 133.62 (×2), 140.81 (×2), 145.18 (×2), 149.57, 152.20, 154.26, 155.64; EI-MS: 356.4 [M+H], 378.4 [M+Na].

4-(7-(3,5-dimethylphenoxy)pyrazolo[1,5-*a*]pyrimidin-5-ylamino)benzonitrile (9a)

Cream white crystal, yield: 24.6%. Mp: 270-272°C; ^{1}H-NMR (DMSO-d_6) δppm: 2.17(s, 6H, CH_3), 5.50 (s, 1H, -CH=), 6.41 (d, 1H, J = 2.1 Hz, -CH=), 7.26-7.34 (m, 3H, benzene), 7.73-7.96 (m, 4H, benzene), 8.09 (d, 1H, J = 2.1 Hz, -CH=), 9.86 (s, 1H, NH); ^{13}C-NMR (DMSO-d_6) δppm: 15.77 (-CH_3 ×2), 119.93 (-CN), Ar-C(×18): 80.00, 94.33, 103.26, 118.73 (×2), 127.57, 130.15 (×2), 130.58 (×2), 133.64 (×2), 145.13, 145.47, 148.63, 149.60, 153.59, 154.40; EI-MS: 356.3 [M+H], 378.4 [M+Na].

4.4 *In vitro* anti-HIV assay

The evaluation of target compounds for their activity against HIV-1 strain III_B and HIV-2 strain ROD in MT-4 cells was performed using the MTT method as previously described [20]. Stock solutions (10 × final concentration) of test compounds were added in 25-µl volumes to two series of triplicate wells to allow simultaneous evaluation of their effects on mock- and HIV-infected cells at the beginning of each experiment. Serial five-fold dilutions of test compounds were made directly in flat-bottomed 96-well microtiter trays by adding 100 µl medium to the 25 µl stock solution and transferring 25 µl of this solution to another well that contained 100 µl medium using a Biomek 3000 robot (Beckman instruments, Fullerton, CA). Untreated control HIV- and mock-infected cell samples were included for each sample.

HIV-1(III_B) [21] or HIV-2 (ROD) [22] stock (50 µL) at 100-300 CCID50 (50%

cell culture infectious dose-50%) or culture medium was added to either the infected or mock-infected wells of the microtiter plate. Mock-infected cells were used to evaluate the effects of test compounds on uninfected cells in order to assess the cytotoxicity of the test compounds. Exponentially growing MT-4 cells were centrifuged for 5 min at 1000 rpm and the supernatant was discarded. The MT-4 cells were resuspended at 6×10^5 cells/mL, and 50-µl volumes were transferred to the microtiter tray wells. Five days after infection, the viability of mock- and HIV-infected cells was examined spectrophotometrically by the MTT assay. The 50% cytotoxic concentration (CC_{50}) was defined as the concentration of the test compound that reduced the viability of the mock-infected MT-4 cells by 50%. The concentration achieving 50% protection from the cytopathic effect of the virus in infected cells was defined as the 50% effective concentration (EC_{50}).

4.5 HIV-RT inhibition assay

Inhibition of HIV-1 RT was performed by using homopolymer template/primer linked to a microplate, biotin-dUTP and RT with detection by ELISA for quantifying expression. The incorporated quantities of the biotin-dUTP into the template represented the activity of HIV-1 RT. IC_{50} values corresponded to the concentration of target compound required to inhibit biotin-dUTP incorporation by 50%. The procedure for assaying RT inhibition was performed as described in the kit (Roche) protocol [18]. A total of 4 ng recombinant HIV-1-RT was added per well. The tested compound **5a** and two control drugs NVP, ETV was used at different concentration gradient (25 µg/mL, 5 µg/mL, 1 µg/mL, 0.2 µg/mL, 0.04 µg/mL for **5a**; 10 µg/mL, 2 µg/mL, 0.4 µg/mL, 0.08 µg/mL, 0.016 µg/mL for NVP; 1µg/mL, 0.2 µg/mL, 0.04 µg/mL, 8.0 ng/mL, 1.6ng/mL for ETV). The percentage inhibition was calculated by formula as given below: inhibition rate = [OD (with RT only)- OD (with RT and inhibitor)]/[OD (with RT only)- OD (without RT and inhibitor)].

Acknowledgments

The financial support from the National Natural Science Foundation of China (NSFC

No. 81273354, No. 81102320, No. 30873133, No.30772629, No. 30371686), Key Project of NSFC for International Cooperation (No. 30910103908), Research Fund for the Doctoral Program of Higher Education of China (No. 20110131130005), Shandong Provincial Natural Science Foundation, China (No. ZR2009CM016) and KU Leuven (GOA 10/014) is gratefully acknowledged. We thank K. Erven, K. Uyttersprot and C. Heens for technical assistance with the HIV assays.

The authors have declared no conflict of interest.

References

[1] B. Hirschel, P. Francioli, Progress and problems in the fight against AIDS, N Engl J Med, 338 (1998) 906-908.

[2] C. Mugnaini, M. Alongi, A. Togninelli, H. Gevariya, A. Brizzi, F. Manetti, C. Bernardini, L. Angeli, A. Tafi, L. Bellucci, F. Corelli, S. Massa, G. Maga, A. Samuele, M. Facchini, I. Clotet-Codina, M. Armand-Ugon, J.A. Este, M. Botta, Dihydro-alkylthio-benzyl-oxopyrimidines as inhibitors of reverse transcriptase: synthesis and rationalization of the biological data on both wild-type enzyme and relevant clinical mutants, J Med Chem, 50 (2007) 6580-6595.

[3] A. Mai, M. Artico, D. Rotili, D. Tarantino, I. Clotet-Codina, M. Armand-Ugoon, R. Ragno, S. Simeoni, G. Sbardella, M.B. Nawrozkij, A. Samuele, G. Maga, J.A. Estee, Synthesis and biological properties of novel 2-Aminopyrimidin-4(3H)-ones highly potent against HIV-1 mutant strains, J Med Chem, 50 (2007) 5412-5424.

[4] J. Guillemont, E. Pasquier, P. Palandjian, D. Vernier, S. Gaurrand, P.J. Lewi, J. Heeres, M.R. de Jonge, L.M.H. Koymans, F.F.D. Daeyaert, M.H. Vinkers, E. Arnold, K. Das, R. Pauwels, K. Andries, M.P. de Bethune, E. Bettens, K. Hertogs, P. Wigerinck, P. Timmerman, P.A.J. Janssen, Synthesis of novel diarylpyrimidine analogues and their antiviral activity against human immunodeficiency virus type 1, J Med Chem, 48 (2005) 2072-2079.

[5] P.A.J. Janssen, P.J. Lewi, E. Arnold, F. Daeyaert, M. de Jonge, J. Heeres, L. Koymans, M. Vinkers, J. Guillemont, E. Pasquier, M. Kukla, D. Ludovici, K. Andries, M.P. de Bethune, R. Pauwels, K. Das, A.D. Clark, Y.V. Frenkel, S.H. Hughes, B. Medaer, F. De Knaep, H. Bohets, F. De Clerck, A. Lampo, P. Williams, P. Stoffels, In search of a novel anti-HIV drug: Multidisciplinary coordination in the discovery of 4-[[4-[[4-[(1E)-2-cyanoethenyl]-2,6dimethylphenyl] amino]-2-pyrimidinyl]amino]-benzonitrile (R278474, rilpivirine), J Med Chem, 48 (2005) 1901-1909.

[6] C.D. Miller, J. Crain, B. Tran, N. Patel, Rilpivirine: a new addition to the anti-HIV-1 armamentarium, Drugs Today (Barc), 47 (2011) 5-15.

[7] J. Girardet, Y. Koh, S. Shaw, H. Kin, WO2006122003A2, 2006.

[8] A. Raney, R. Hamatake, W. Xu, J.-L. Girardet, J.-M. Vernier, L.-T. Yeh, B. Quart, A novel NNRTI class with potent Anti-HIV activity against NNRTI-resistant viruses, 21st International Conference on Antiviral ResearchMontreal, Quebec, Canada, 2008.

[9] A. Raney, R. Hamatake, W. Xu, J.-M. Vernier, J.-L. Girardet, P. Weingarten, D. Zhou, H.K. Kim, R. Dick, L.-T. Yeh, B. Quart, RDEA427 and RDEA640 are Novel NNRTIs with Potent Anti-HIV Activity Against NNRTI-Resistant Viruses, 15st Conference on Retroviruses and Opportunistic InfectionsBoston, MA, USA, 2008.

[10] Y. Tian, D. Rai, P. Zhan, C. Pannecouque, J. Balzarini, E. Clercq, H. Liu, X. Liu, Design, synthesis and biological evaluation of novel 3,5-disubstituted-1, 2,6-thiadiazine-1,1-dione derivatives as HIV-1 NNRTIs, Chemical biology & drug design, (2013).

[11] X. Chen, P. Zhan, D. Li, E.D. Clercq, X. Liu, Recent advances in DAPYs and related analogues as HIV-1 NNRTIs, Curr Med Chem, 18 (2011) 359-376.

[12] X. Chen, P. Zhan, X. Liu, Z. Cheng, C. Meng, S. Shao, C. Pannecouque, E.D. Clercq, X. Liu, Design, synthesis, anti-HIV evaluation and molecular modeling of piperidine-linked amino-triazine derivatives as potent non-nucleoside reverse transcriptase inhibitors, Bioorganic & Medicinal Chemistry, 20 (2012) 3856-3864.

[13] D. Li, P. Zhan, H. Liu, C. Pannecouque, J. Balzarini, E. De Clercq, X. Liu, Synthesis and biological evaluation of pyridazine derivatives as novel HIV-1 NNRTIs, Bioorganic & medicinal chemistry, (2013).

[14] C.S. Alvarez, T.Y. Chan, L.W. Dillard, R.J. Doll, M.P. Dwyer, T.O. Fischmann, V.M. Girijavallabhan, T.J. Guzi, Z.M. He, R.A. James, WO2004026229A2, 2004.

[15] D.S. Williamson, M.J. Parratt, J.F. Bower, J.D. Moore, C.M. Richardson, P. Dokurno, A.D. Cansfield, G.L. Francis, R.J. Hebdon, R. Howes, Structure-guided design of pyrazolo [1, 5-a] pyrimidines as inhibitors of human cyclin-dependent kinase 2, Bioorganic & medicinal chemistry letters, 15 (2005) 863-867.

[16] T. Kosugi, D.R. Mitchell, A. Fujino, M. Imai, M. Kambe, S. Kobayashi, H. Makino, Y. Matsueda, Y. Oue, K. Komatsu, K. Imaizumi, Y. Sakai, S. Sugiura, O. Takenouchi, G. Unoki, Y. Yamakoshi, V. Cunliffe, J. Frearson, R. Gordon, C.J. Harris, H. Kalloo-Hosein, J. Le, G. Patel, D.J. Simpson, B. Sherborne, P.S. Thomas, N. Suzuki, M. Takimoto-Kamimura, K. Kataoka, Mitogen-Activated Protein Kinase-Activated Protein Kinase 2 (MAPKAP-K2) as an Antiinflammatory Target: Discovery and in Vivo Activity of Selective Pyrazolo(1,5-a)pyrimidine Inhibitors Using a Focused Library and Structure-Based Optimization Approach, J Med Chem, 55 (2012) 6700-6715.

[17] X. Ma, S. Yang, S. Gu, Q. He, F. Chen, E. De Clercq, J. Balzarini, C. Pannecouque, Synthesis and Anti-HIV Activity of Aryl-2-[(4-cyanophenyl)amino]-4-pyrimidinone hydrazones as Potent Non-nucleoside Reverse Transcriptase Inhibitors, ChemMedChem, 6 (2011) 2225-2232.

[18] Reverse Transcriptase Assay, Colorimetric. Roche Diagnostics GmbH, Roche Applied Science., Version 13.0 ed.2010.

[19] C.A. Lipinski, F. Lombardo, B.W. Dominy, P.J. Feeney, Experimental and computational approaches to estimate solubility and permeability in drug discovery and development settings, Advanced drug delivery reviews, (2001).

[20] C. Pannecouque, D. Daelemans, E. De Clercq, Tetrazolium-based colorimetric assay for the detection of HIV replication inhibitors: revisited 20 years later, Nat. Protocols, 3 (2008) 427-434.

[21] M. Popovic, M. Sarngadharan, E. Read, R. Gallo, Detection, isolation, and continuous production of cytopathic retroviruses (HTLV-III) from patients with AIDS and pre-AIDS, Science, 224 (1984) 497-500.

[22] F. Clavel, D. Guetard, F. Brun-Vezinet, S. Chamaret, M. Rey, M. Santos-Ferreira, A. Laurent, C. Dauguet, C. Katlama, C. Rouzioux, e. al., Isolation of a new human retrovirus from West African patients with AIDS, Science, 233 (1986) 343-346.

Captions:

Figure 1. Representative analogues of the DAPY series.

Figure 2. Structure-based biosterism design of 5,7-disubstituted pyrazolo[1,5-*a*]pyrimidine derivatives as HIV-1 NNRTIs.

Scheme 1. The synthetic route for pyrazolo[1,5-*a*]pyrimidine derivatives.

Table 1. Inhibitory action of compounds **4a-g**, **5a-g**, **6a**, **7a**, **8a**, **9a** against HIV replication and cytotoxicity in MT-4 cells.

Table 2. Activity of pyrazolo[1,5-*a*]pyrimidine derivative **5a** against HIV-1 RT.

Table 3. Docking scores[a] of TMC125, RDEA640 and **5a** by Surflex-Dock.

Figure 3. Docking of **5a** is shown by Pymol (version: 0.99rc6): (a) Molecular superposition of **5a** (carbon atoms in yellow) with TMC125 (original ligand extracted from 3MEC, carbon atoms in gray; newly docked molecule as the reference, carbon atoms in pink) and RDEA640 (carbon atoms in salmon) in the binding site; (b) Molecular model of **5a** in the RT non-nucleoside binding site (PDB code: 3MEC).

Table 4. Physicochemical properties[a] of **5a**, ETV and NVP.

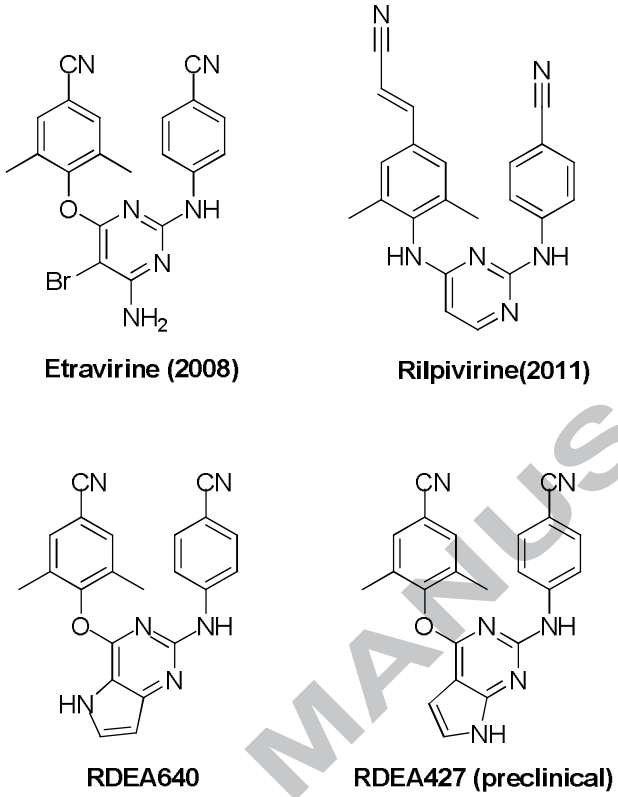

Figure 1. Representative analogues of the DAPY series

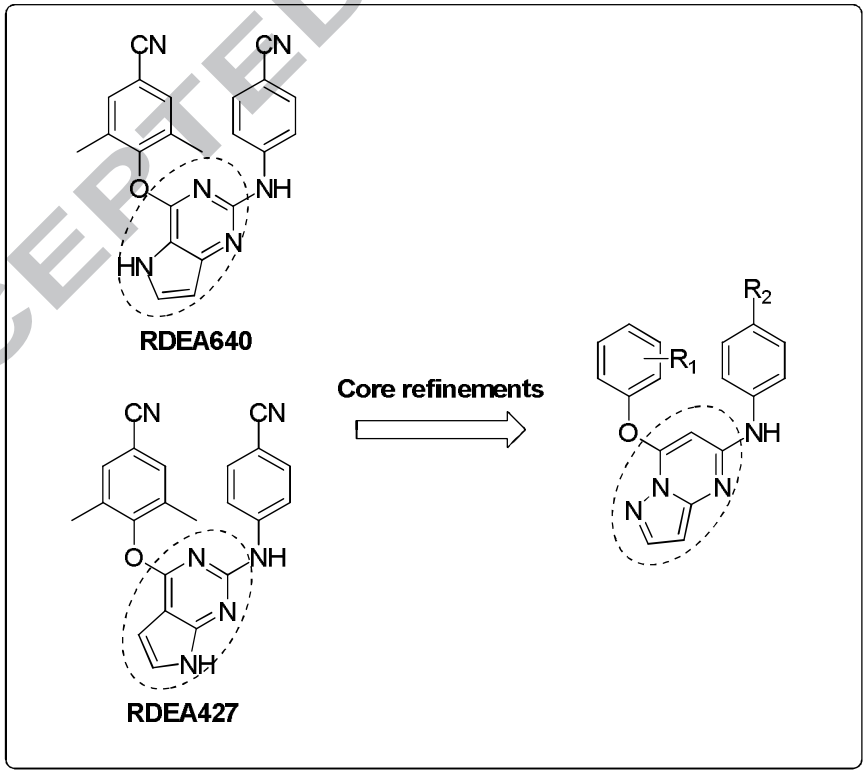

Figure 2. Structure-based biosterism design of 5,7-disubstituted pyrazolo[1,5-*a*]pyrimidine derivatives as HIV-1 NNRTIs

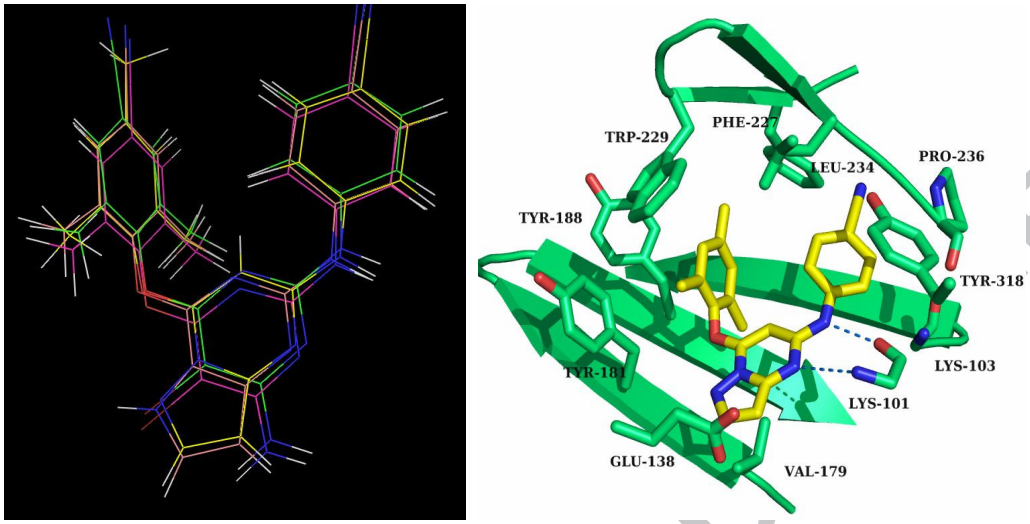

(a) (b)

Figure 3. Docking of **5a** is shown by Pymol (version: 0.99rc6): (a) Molecular superposition of **5a** (carbon atoms in yellow) with TMC125 (original ligand extracted from 3MEC, carbon atoms in gray; newly docked molecule as the reference, carbon atoms in pink) and RDEA640 (carbon atoms in salmon) in the binding site; (b) Molecular model of **5a** in the RT non-nucleoside binding site (PDB code: 3MEC).

Sheme 1

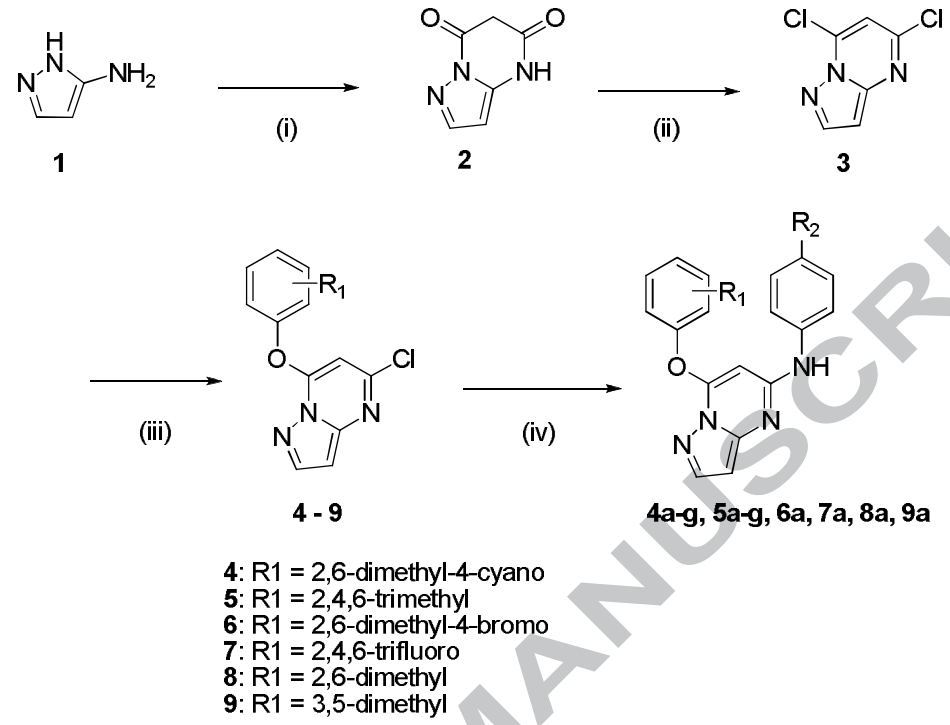

Scheme 1. The synthetic route for pyrazolo[1,5-*a*]pyrimidine derivatives.

Table 1. Inhibitory action of compounds **4a-g**, **5a-g**, **6a**, **7a**, **8a**, **9a** against HIV replication and cytotoxicity in MT-4 cells.

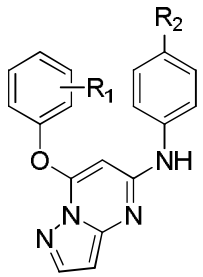

Pyrazolo[1,5-a]pyrimidine series

Compd	R_1	R_2	EC_{50}(μM)[a]		CC_{50}(μM)[b]	SI[c]	
			HIV-1 III_B	HIV-2 ROD		HIV-1 III_B	HIV-2 ROD
4a	2,6-Dimethyl-4-Cyano	4-Cyano	1.52±0.17	>181	181±26.74	120	<1
4b	2,6-Dimethyl-4-Cyano	4-Bromo	1.60±0.65	>8.51	8.51±8.08	5	<1
4c	2,6-Dimethyl-4-Cyano	4-Chloro	1.13±0.11	>13.3	13.3±10.8	12	<1
4d	2,6-Dimethyl-4-Cyano	4-Fluoro	3.09±0.72	>33.6	33.6±2.16	11	<1
4e	2,6-Dimethyl-4-Cyano	4-Methyl	0.46±0.15	>10.8	10.8±10.7	23	<1
4f	2,6-Dimethyl-4-Cyano	4-Methoxy	0.91±0.43	>280	≥280	≥308	<orX1
4g	2,6-Dimethyl-4-Cyano	4-Nitro	4.04±0.50	>229	229±23.1	57	<1
5a	**2,4,6-Trimethyl**	**4-Cyano**	**0.07±0.01**	**>276**	**276±53.7**	**3999**	**<1**
5b	2,4,6-Trimethyl	4-Bromo	0.14±0.09	>122	122±15.3	854	<1
5c	2,4,6-Trimethyl	4-Chloro	0.17±0.08	>139	139±26.8	814	<1
5d	2,4,6-Trimethyl	4-Fluoro	0.73±0.55	>289	289±59.8	397	<1
5e	2,4,6-Trimethyl	4-Methyl	0.17±0.12	>157	157±23.9	950	<1
5f	2,4,6-Trimethyl	4-Methoxy	0.28±0.09	>334	>334	>1178	X1
5g	2,4,6-Trimethyl	4-Nitro	0.69±0.42	>321	>321	>466	X1
6a	2,6-Dimethyl-4-Bromo	4-Cyano	0.49±0.23	>266	266±47.5	544	<1
7a	2,4,6-Trifluoro	4-Cyano	5.98±2.34	>45.4	45.4±7.65	8	<1
8a	2,6-Dimethyl	4-Cyano	>188	>188	188±11.4	<1	<1
9a	3,5-Dimethyl	4-Cyano	5.11±2.53	>47.7	47.7±9.87	9	<1
NVP	-	-	0.17±0.06	-	>14.99	>89	-
DLV	-	-	0.16±0.15	-	>43.81	>277	-
ETV[d, 14]	-	-	0.003	0.011	>4.6	>1537	>412

[a] EC_{50}: concentration of compound required to achieve 50% protection of MT-4 cells against HIV-1-induced cytopathic effect, as determined by the MTT method;

[b] CC_{50}: concentration required to reduce the viability of mock-infected cells by 50%, as determined by the MTT method;

[c] SI: selectivity index (CC_{50}/EC_{50}), and the SI values: X1 stands for ≥1 or <1 .

[d] The data were obtained from the same lab of the Rega Institute for Medical Research, KU Leuven, Belgium.

Table 2. Activity of pyrazolo[1,5-*a*]pyrimidine derivative **5a** against HIV-1 RT.

Compound	**5a**	**NVP**	**ETV**
IC_{50}[a]	2.26 μM	0.55 μM	0.083 μM

[a] IC_{50}: inhibitory concentration required to inhibit biotin deoxyuridine triphosphate (biotin-dUTP) incorporation into poly [A] × oligo $[dT]_{15}$ by the HIV-1 RT by 50% (RT kit, Roche).

Table 3. Docking scores[a] of TMC125, RDEA640 and **5a** by Surflex-Dock.

Comp.	**T_S**	**C**	**P**	**R**	**S**	**D_S**	**P_S**	**G_S**	**CHS**	**CS**	**G_C**
TMC125	10.15	-0.84	1.64	0.47	0.96	-175.69	-103.11	-321.527	-36.02	5	5
RDEA640	10.11	-1.19	1.39	1e+006	0.80	-175.64	-101.15	-326.61	-37.62	5	5
5a	8.99	-2.22	1.30	1e+006	0.83	-173.76	-82.34	-323.61	-39.38	5	5

[a] T_S = Total_ score; C = Crash; P = Polar; R = RMSD_ISO; S = Similarity; D_S = D_SCORE; P_S = PMF_SCORE; G_S = G_SCORE; CHS = CHEMSCORE, CS = CSCORE, G_S = GLOBAL_CSCOR.

Table 4. Physicochemical properties[a] of **5a**, ETV and NVP.

Compd.	**EC_{50}(μM)**	**nViol**	**natoms**	**miLogP**	**MW**	**nON**	**nOHNH**	**nrotb**	**TPSA**	**MV**
Acceptable range				(< 5)	(<500 Da)	<10	<5		(<140Å)	
5a	0.07	1	28	5.741	369.43	6	1	4	75.25	335.87
ETV	0.003[b, 14]	1	28	5.027,	435.28	7	3	4	120.65	335.95
NVP	0.17	0	20	1.385	266.30	5	1	1	63.58	236.62

[a] nViol = number of violations; natoms = no. of atoms; miLog P = molinspiration predicted Log P; MW = molecular weight; nON = no. of hydrogen bond acceptors; nOHNH = no. of hydrogen bond donors; nrotb = no. of rotatable bonds; TPSA= topological polar surface area; MV = molar volume.

[b] The data were obtained from the Rega Institute for Medical Research, KU Leuven, Belgium).

Graphical Abstract:

A novel class of 5,7-disubstituted pyrazolo[1,5-*a*]pyrimidine derivatives were rationally designed, synthesized and evaluated for their anti-HIV activities in MT4 cell cultures.

5,7-Disubstituted pyrazolo[1,5-*a*]pyrimidine derivatives as potent HIV-1 NNRTIs

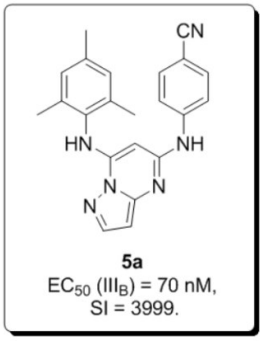

5a
EC_{50} (III_B) = 70 nM,
SI = 3999.